Neurobiology of Disease 125 (2019) 219–231

Contents lists available at ScienceDirect

Neurobiology of Disease

journal homepage: www.elsevier.com/locate/ynbdi

# Olfactory bulb atrophy and caspase activation observed in the BACHD rat models of Huntington disease

M. Lessard-Beaudoin[a,1], L. Yu-Taeger[b,c,1], M. Laroche[a], E. Singer[b], O. Riess[b], H.H.P. Nguyen[b,c], R.K. Graham[a,*]

[a] Research Center on Aging, Department of Pharmacology and Physiology, University of Sherbrooke, Sherbrooke, Canada
[b] Institute for Medical Genetics and Applied Genomics, University of Tuebingen, Tuebingen, Germany
[c] Department of Human Genetics, Ruhr University, Bochum, Germany

ARTICLE INFO

*Keywords:*
Caspases
Olfactory system
Apoptosis
Huntington disease
BACHD rats

ABSTRACT

Olfactory dysfunction is observed in several neurological disorders, including Huntington disease (HD), and correlates with global cognitive performance, depression and degeneration of olfactory regions in the brain. Despite clear evidence demonstrating olfactory dysfunction in HD patients, only limited details are available in murine models and the underlying mechanisms are unknown. In order to determine if alterations in the olfactory bulb (OB) are observed in HD we assessed OB weight or area from 3 to 12 months of age in the BACHD transgenic lines (TG5 and TG9). A significant decrease in the OB was observed at 6 and 12 months of age compared to WT. We also detected increased mRNA and protein expression of mutant huntingtin (mHTT) in the OB of TG5 compared to TG9 at specific ages. Despite the higher expression of mHTT in the TG5 OBs, there was increased nuclear accumulation of mHTT in the OB of TG9 compared to WT and TG5 rats. As we observed atrophy of the OB in the BACHD rats we assessed for caspase activation, a known mechanism underlying the cell death observed in HD. We characterized caspase-3, −6, −8 and − 9 mRNA and protein expression levels in the OB of the BACHD transgenic lines at 3, 6 and 12 months of age. Alterations in caspase mRNA and protein expression were detected in the TG5 and TG9 lines. However, the changes observed in the mRNA and protein levels are in some cases discordant, suggesting that the caspase protein modifications detected may be more attributable to post-translational modifications. The caspase activation studies support that cell death may be increased in the rodent HD OB and further our understanding of the olfactory dysfunction and the role of caspases in the pathogenesis of HD.

## 1. Introduction

Huntington disease (HD), an autosomal dominant neurodegenerative disease caused by expansion of CAG repeats in exon 1 of the HD gene named as *HTT*, results in motor (Jankovic and Roos, 2014), cognitive and psychiatric symptoms (Burns et al., 1990; Cummings, 1995; Ross et al., 2014). Furthermore, substantial data in the literature demonstrates that olfactory dysfunction is observed in HD (Bylsma et al., 1997; Hamilton et al., 1999; Larsson et al., 2006; Nordin et al., 1995; Tabrizi et al., 2009) and indeed that it may be an early symptom and prior to the onset of motor symptoms (Moberg et al., 1987; Paulsen et al., 2008; Paulsen et al., 2014; Pirogovsky et al., 2007; Tabrizi et al., 2009). The olfactory deficits observed in HD include a decrease in olfactory sensitivity, odor discrimination, odor recognition memory and odor identification ability compared to healthy controls (Bacon Moore et al., 1999; Moberg and Doty, 1997; Moberg et al., 1987; Nordin et al., 1995). Moreover, in HD patients, the quality of odor discrimination negatively correlates with the number of CAG repetitions in the HD gene (Larsson et al., 2006). Olfactory dysfunction is also observed in other neurodegenerative diseases and is accompanied by structural abnormalities of the olfactory epithelium, the olfactory bulb (OB) and the olfactory cortices (Barresi et al., 2012; Doty, 2012a; Menalled et al.,

*Abbreviation:* HD, Huntington disease; BAC, Bacterial artificial chromosome; OB, olfactory bulb; HTT, huntingtin; mHTT, mutant huntingtin; WT, wild-type; Trp, transient Receptor Potential; GCL, granule cell layer; IPL, internal plexiform layer; EPL, external plexiform layer; MCL, mitral cell layer; GL, glomerular layer.

* Corresponding author at: Department of Pharmacology and Physiology, Faculty of Medicine and Health Sciences, Research Centre on Aging, University of Sherbrooke, 3001 12e Avenue Nord, Sherbrooke J1H 5N4, Canada.
*E-mail address:* Rona.Graham@USherbooke.ca (R.K. Graham).

[1] M.L.B and Y-T. L contributed equally to this work.

https://doi.org/10.1016/j.nbd.2019.02.002
Received 9 July 2018; Received in revised form 14 December 2018; Accepted 4 February 2019
Available online 06 February 2019

2003; Thomann et al., 2009; Youssef et al., 2008).

Olfactory system deficits are also observed in murine models of HD and include decreases in olfactory sensitivity (R6/1) and olfactory discrimination (HdhQ111) in the early and late stages of the disease (Holter et al., 2013; Mo et al., 2015). Furthermore, activation of brain regions in response to an olfactory stimulus shows a gene dose effect in the HD knock-in mouse model (Ferris et al., 2014). In the YAC128 HD mice, a decrease has been observed in the olfactory bulb volume (Carroll et al., 2011), an area which has previously been reported to correlate with olfactory functions (Buschhuter et al., 2008; Hummel et al., 2011).

Mutant huntingtin (mHTT) aggregates have also been detected in several olfactory regions in the HD human and rodent brain (Hamilton et al., 1999; Kohl et al., 2010; Menalled et al., 2003). One of the primary functions of the OB is the generation of new neurons, thus the olfactory deficits observed in HD may be an early sign of a defect in neurogenesis and potentially be involved in the neurodegenerative processes. Indeed, impaired neurogenesis is observed in human and murine HD brain (Curtis et al., 2003; Curtis et al., 2005; Fedele et al., 2011; Kohl et al., 2010; Lazic et al., 2007), and other neurodegenerative conditions (Han et al., 2016; Wirths, 2017).

Several models of HD have been created in order to reproduce the symptoms of the disease with the most fidelity. Among them, the BACHD rats display a robust, early onset and progressive HD-like phenotype including motor deficits and anxiety-related symptoms (Abada et al., 2013; Yu-Taeger et al., 2012). There are two lines characterized (TG5 and TG9) and both express the complete human m*HTT* sequence, including regulatory elements and the human *HTT* promoter. Overall, the TG5 line expresses higher levels of mHTT (in copy number, mRNA and protein) in the whole brain and presents with motor deficits on the accelerated rotarod test by 1 month of age (Yu-Taeger et al., 2012). An abnormal walking strategy is observed at 3 months in line TG5 and at 5 months in TG9 line consistent with the mHTT dosage effect (Yu-Taeger et al., 2012).

Several proteases (caspase-1, -3, -6, -7 et -8, calpains and aspartyl-proteases) have been shown to cleave HTT both in vitro and in vivo and the resulting fragments containing the expanded polyglutamine repeat are found in human and rodent HD brain (Gafni et al., 2004; Goldberg et al., 1996; Hermel et al., 2004a; Kim et al., 2002; Lunkes et al., 2002; Mende-Mueller et al., 2001; Wellington et al., 2002b). Caspase activation, in particular caspase-6, is known to be a critical step in the pathogenesis of HD. Mice expressing mHTT resistant to cleavage by caspase-6, maintain normal neuronal function and do not develop striatal neurodegeneration (Graham et al., 2010; Graham et al., 2012; Graham et al., 2006a; Metzler et al., 2010; Milnerwood et al., 2010; Pouladi et al., 2009). Alterations of other caspases have also been implicated in the pathogenesis of HD including caspase-3, -8, -9 and -10, and in other expanded polyglutamine diseases (Gervais et al., 2002; Kiechle et al., 2002; Rigamonti et al., 2001; Sanchez et al., 1999b; Toulmond et al., 2004; U et al., 2001). Importantly, caspase activity has been shown to be an essential step in maintaining the normal turnover of OB cells through neurogenesis (Mouret et al., 2009). As caspases are key components in the pathogenesis of HD, and the functions related to the OB are impaired in the disease, we assessed OB weight and caspase expression profiles in the OB of the two lines of the BACHD (TG5 and TG9) rodent model in order to determine if activation of caspases may provide an explanation for the olfactory dysfunction and olfactory system atrophy observed in HD.

## 2. Material and methods

### 2.1. Animals

The olfactory bulbs (OB) were collected from two lines of the BACHD rat model (TG5 and TG9), transgenic rat models expressing human mutant full-length *HTT* gene with 97 CAG/CAA repeats, at 3, 6 and 12 months of age (Yu-Taeger et al., 2012). The rats were fed ad libitum and kept in a normal light and dark cycle. All experiments were approved by the local ethics committee at Regierungspraesidium Tuebingen (HG2/10), and carried out in accordance with the German Animal Welfare Act and the guidelines of the Federation of European Laboratory Animal Science Associations, based on European Union legislation (Directive 2010/63/EU).

### 2.2. Quantification of OB weight and area

The weight of the OBs of the BACHD rats and WT rats were obtained using an analytic balance (Denver instrument, SI-64) at 3 and 6 months of age. The area of the OB of the BACHD rats and WT rats were assessed at 12 months of age as following: rats were perfused with 4% paraformaldehyde in saline buffer followed by post-fixation of the brains in the same fixative. Nissl staining was performed to visualize different layers of the OB using 40-µm thick coronal cryosections. Three olfactory bulb sections with 960 µm intervals were chosen for the quantification of the OB area. We analyzed three areas separately: i) the total area of the mitral cell layer (MCL), internal plexiform layer (IPL) and granule cell layer (GCL); ii) area of the external plexiform layer (EPL); iii) area of the glomerular layer (GL). The region of interest (ROI) of the MCL + IPL + GCL was outlined along the outer edge of MCL of the OB and images were acquired. The area was determined using ImageJ. The area of the EPL was assessed by subtracting the total area of MCL + IPL + GCL from the area outlined along the outer edge of EPL. The area of the GL was calculated by subtracting the area outlined along the outer edge of EPL from the area outlined along the outer edge of GL. The area values of the three sections of each animal were averaged and compared among the groups.

### 2.3. Real-Time Quantitative RT-PCR

Total RNA was extracted from the OBs with RNeasy mini kit (QIAGEN) and cDNA was prepared using ProtoScript Reverse transcriptase II (#M0368X, New England BioLabs). Quantification was done using Mx3005P QPCR Systems (Stratagene) with rat-specific primers for caspase-3 (Forward: 5′-GGACCTGTGGACCTGAAAAA-3′; Reverse: 5′-GCATGCCATATCATCGTCAG-3′), caspase-6 (Forward: 5′-ACGTGGT GGATCATCAGACA-3′; Reverse: 5′-GGAGCCGTTCACAGTCTCTC-3′), caspase-8 (Forward: 5′-GGGGATGGCTACTGTGAAAA-3′; Reverse: 5′-CATGTTCCTCGGGTTGTCTT-3′), caspase-9 (Forward: 5′-AAGACCA TGGCTTTGAGGTG-3′; Reverse: 5’-CAGGAACCGCTCTTCTTGTC-3′), and PgK1 (Forward: 5′-CCAAACAATCTGCTTAGCTCG-3′, Reverse: 5′-GATGAGAATGCAAAGACTGGC-3′). The primers designed to quantify transgenic mutant HTT were (Forward: 5’-ATCTTGAGCCACAGCT CCAGCCA-3′; Reverse: 5′-GGCCTCCGAGGCTTCATCAGG-3′) and the primers used to quantify endogenous rat HTT were (Forward: 5′-ATC TTGAGCCACAGCTCCAGCCA-3′; Reverse: 5′-TCTGAAAACGTCTGAGA CTTCACCAGA-3′). Amplification of the references gene PgK1 was used to standardize the amount of sample RNA in the reaction. Gene-expression levels were measured using MxPro QPCR Software (Stragene).

### 2.4. Western blot analysis

OBs were homogenized and sonicated in lysis buffer (0.32 mM Sucrose, 20 mM Tris pH 7.2, 1 mM $MgCl_2$, 0.5 mM EDTA pH 7.2) using a cocktail of protease inhibitors (Roche), PefaBloc SC (Roche) and *Z*-VAD-fmk (Enzo Lifes Sciences) and clarified by centrifugation at 13,000 rpm. The protein concentration was determined using the BCA (bicinchoninic acid) protein assay kit (Pierce). Protein lysates (50 µg) were separated on 10% or 4–15% gels and transferred to PVDF membrane (PerkinElmer). The membranes were probed with caspase-3 (Cell Signalling, 9662, dilution: 1/1000), caspase-6 (Cell Signalling, 9762, dilution: 1/500), caspase-8, (Santa Cruz, sc-7890, dilution: 1/100), caspase-9 (Cell Signalling, 9508, dilution: 1/1000), huntingtin

(Millipore, MAB2166, dilution 1:500), Polyglutamine-Expansion disease marker (Millipore, 1:3000, MAB1574), Calnexin (Abcam, 1:2000, ab75801) or actin (Millipore, MAB1501, dilution 1/10000) antibodies. Peroxidase activity was detected and densitometry values were obtained with Odyssey Fc imaging system (Licor) using Luminata Crescendo Western HRP substrate (Millipore). Quantification of β-actin or calnexin was used to standardize the amount of protein in each lane.

### 2.5. HTT immunohistochemistry

Nuclear accumulation of mHTT was investigated by immunohistological staining using the antibody S830, a polyclonal antibody raised against HTT exon 1 recombinant protein with 53Q (kindly provided by Prof. Gillian P. Bates) (Sathasivam et al., 2001). Rat OB sections of two BACHD lines (TG5 and TG9) at 3, 6, 9 and 12 months of age were stained as described previously (Yu-Taeger et al., 2012). Sections were counterstained with thionin to visualize nuclei.

## 3. Results

### 3.1. Atrophy of the olfactory bulb in the BACHD transgenic lines

We assessed OB weight in the BACHD rats (TG5 and TG9) and WT rats at 3 and 6 months of age. A genotype effect was detected which showed a significantly lower OB weight in the TG5 rats (44%), and a trend decrease in the TG9 rats (34%), at 6 months of age compared to WT (Two-way ANOVA: interaction: $p = 0.16$; Age: $p = 0.71$; Genotype: $p = 0.002$; post hoc, 6 months WT vs. TG5, $p < 0.01$; Fig. 1A). A trend decrease is also observed at 3 months of age in TG5 OB compared with WT (*t*-test, $p < 0.01$). We also assessed specific areas within the OB including the i) MCL + IPL + GCL, ii) EPL and iii) GL at 12 months of age. An interaction between the genotypes and the OB layers was observed; suggesting that expression of mHTT may influence the size of specific layers in the OB (two-way ANOVA, Interaction $p = 0.004$; Genotype, $p < 0.0001$; Layers, $p < 0.0001$; Fig. 1B, C). Similar to the OB weight at 6 months of age, we observed a decreased area of the MCL, IPL and GCL in the TG5 and TG9 compared to WT (post hoc IPL and GCL: WT vs. TG5, $p < 0.0001$, WT vs. TG9, $p < 0.01$; Fig. 1C), while the area of the EPL was only decreased in TG5 compared to both WT (post hoc test, $p < 0.0001$) and TG9 rats (post hoc test, $p < 0.01$) (Fig. 1C). No variation in the glomerular layer was observed in either line compared to WT. As we observed a decrease in OB weight, using western blot analysis, we then evaluate the expression of NeuN, a marker of mature neurons. We observed a trend decrease in both lines in NeuN expression (data not shown, t-test WT vs. TG5, $p = 0.09$; WT vs. TG9, $p = 0.08$).

### 3.2. Differential HTT expression profiles between TG5 and TG9 BACHD rats

Strong evidence has demonstrated the opposing effects of wild-type and mutant HTT on cell death and neurogenesis pathways. Indeed, wild-type HTT plays a role in development, neurogenesis, anti-apoptotic pathways, protection against excitotoxic stress, and has been shown to reduce mutant HTT toxicity (Cattaneo et al., 2005; Gervais et al., 2002). As mutant HTT has a dose-dependent (de Almeida et al., 2002; Graham et al., 2006b; Hodgson et al., 1999; Reddy et al., 1998; Squitieri et al., 2003) and opposing effect vs. wild-type HTT, their expression levels may affect the OB atrophy differentially. We therefore evaluated *HTT* mRNA and protein expression levels of both mutant and wild-type HTT in these two lines at 3, 6 and 12 months of age. No difference in wild-type *HTT* OB mRNA levels were observed between BACHD rats and WT rats at any time points assessed (Fig. 2A, B, C). However, a trend increase in the mRNA expression of the HD gene was observed in TG9 rats compared to WT at 12 months (*t*-test: $p < 0.05$, Fig. 2C). The real-time quantification PCR analysis also revealed higher expression of *mHTT* mRNA in the OB of the TG5 rats compared to TG9 at 3 months (ANOVA, $p < 0.001$, Fig. 2D) and 12 months of age (ANOVA, $p < 0.05$, Fig. 2F). Although we did not detect any significant variation in mRNA levels of wild-type *HTT* in the OB at 3 months of age between genotypes, we did detect a decrease in wild-type HTT protein expression in TG9 vs. WT rats at that age (ANOVA $p = 0.016$, post hoc, $p < 0.05$, Fig. 3A, B, Sup. Fig 1). Correlating with the *mHTT* mRNA results at 3 months of age, we detected increased OB mHTT protein levels in TG5 compared to TG9 at this time point (ANOVA, Fig. 3C-E, Sup. Fig. 1). At 6 and 12 months of age, no difference in endogenous or mHTT protein expression levels was observed between TG5 and TG9 (Fig. 3F-L, Sup. Fig. 1). However, the mHTT/wild-type HTT ratio in the OB of TG5 rats was increased compared to TG9 at 3 and 12 months of age (Fig. 3E *t*-test, $p < 0.0001$, M t-test, $p < 0.001$, Sup. Fig. 1).

Despite the higher protein expression of mHTT in TG5 rats compared to the TG9 at 3 months of age, nuclear accumulation of mHTT, assessed using the S830 antibody, was observed earlier in the TG9 OB (3 months of age) compared to TG5 rats (6 months of age) (Fig. 4). By the age of 9–12 months, TG9 rats clearly display more intense nuclear immunoreactivity of mHTT in the OB than TG5 (Fig. 4). The quantification of mHTT nuclear accumulation shows an interaction by two-way ANOVA indicating that the increase in the nuclear immunostaining of mHTT occurs earlier in TG9 OB compared to TG5 (two-way ANOVA,Interaction, $p < 0.0001$: Genotype, $p < 0.0001$, Age $p < 0.0001$. Of note, the nuclear accumulation was almost exclusively observed in the IPL, GCL and MCL of the OB (Fig. 4, Sup. Fig. 2).

### 3.3. Increase in mRNA levels of specific caspases in BACHD olfactory bulb

As we observed atrophy of the OB in the BACHD lines, we next performed a temporal investigation of caspase expression profiles in the OB of the BACHD TG5 and TG9 rats. At 6 and 12 months of age, an increase in caspase-3 mRNA expression levels was observed in the OB of the TG9 rats compared to WT (6 months: ANOVA $p = 0.03$, post hoc: WT vs TG9 $p < 0.05$, TG5 vs TG9, $p < 0.05$; Fig. 5C, 12 months: ANOVA $p = 0.02$, post hoc: WT vs TG9 $p < 0.05$, Fig. 5B-C). Furthermore, an increase in the expression of caspase-6 mRNA was observed in the OB of TG9 rats compared to WT at 3 months of age (ANOVA $p = 0.059$, *t*-test: WT vs TG9 $p < 0.05$, Fig. 5D). However, at 6 and 12 months, no difference between genotype was observed (Fig. 5E-F). No variation in caspase-8 mRNA expression levels was detected between the BACHD lines and WT OB at any age (Fig. 5G-I). In contrast to the increased mRNA expression observed for caspase-3 and -6 in TG9 OB, a decrease in caspase-9 mRNA expression was observed in TG5 OB at 6 months of age compared to WT OB (ANOVA $p = 0.04$, post hoc: WT vs. TG5, $p < 0.05$, Fig. 5K) and there was a trend decrease in caspase-9 in TG9 OB at 3 months of age (ANOVA $p = 0.08$, *t*-test: TG5 vs TG9, $p < 0.05$, Fig. 5J).

### 3.4. Alterations in caspase protein expression profiles in BACHD olfactory bulb

At the protein level, the p30 and p19 fragments of caspase-3 tend to increase in the TG9 OB compared to WT at 3 months of age, while no further variation was observed at 6 and 12 months of age (p30: ANOVA $p = 0.07$; p19: ANOVA $p = 0.09$, Fig. 6A-C, Sup. Fig. 3). While no change in the percentage of active caspase-3 was detected by ANOVA at 3 months of age between genotypes, a trend increase in active caspase-3 was observed in TG9 OB compared to WT (*t*-test, $p < 0.05$, Sup. Fig. 4). Furthermore, there was a significant decrease in the caspase-6 p20p10 fragment, an intermediate fragment in the path of activation, in both TG5 and TG9 OB, and a trend decrease in the caspase-6 proform in TG5 OB compared to WT at 3 months (Proform: ANOVA $p = 0.09$, t-test: WT vs. TG5 $p < 0.05$; p20p10: ANOVA $p = 0.003$, post hoc: WT vs. TG5, $p < 0.05$; WT vs. TG9, $p < 0.05$, Fig. 6D, Sup. Fig. 3). Despite

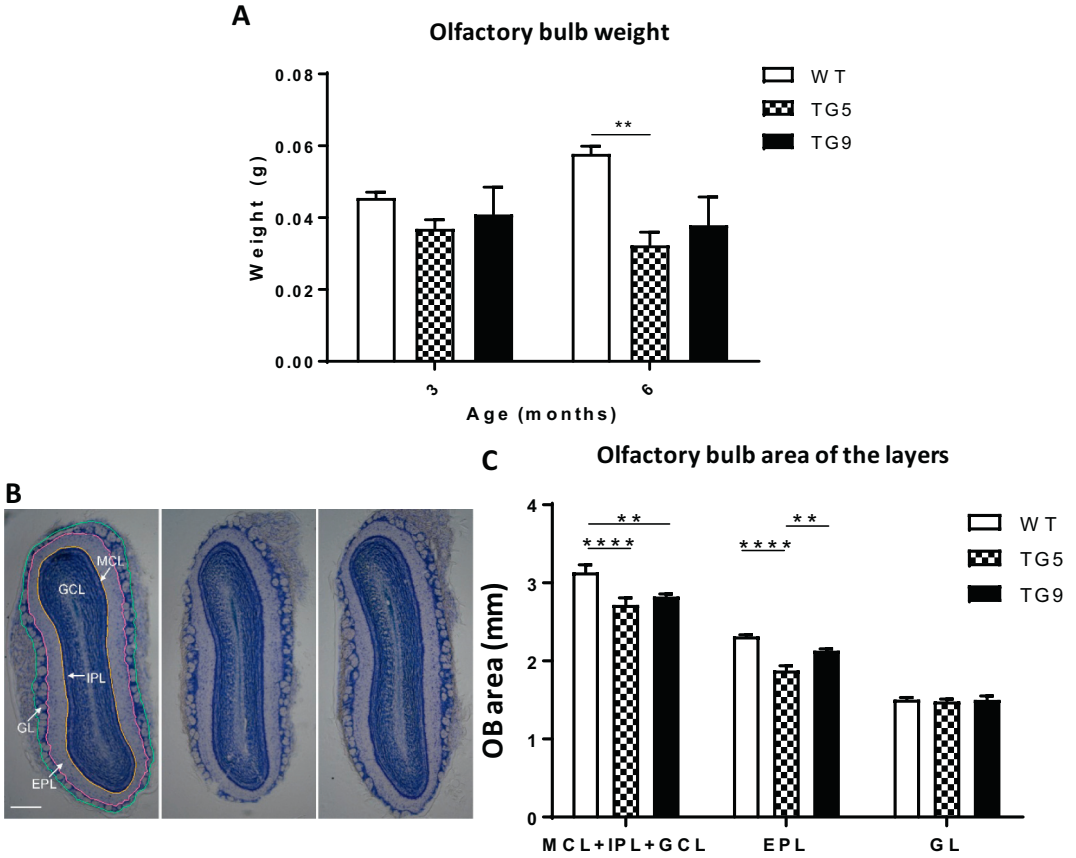


**Fig. 1.** Atrophy of the olfactory bulb in BACHD rodents. A) A significant effect of genotype showing a global decrease in olfactory bulb (OB) weight is observed in BACHD rats at 6 months of age compared to WT rats (Two-way ANOVA: Interaction p = 0.16, Age p = 0.71, Genotype p = 0.002.; 3 months: WT $n$ = 10, TG5 $n$ = 8 and TG9 $n$ = 9; 6 months: WT n = 8, TG5 $n$ = 6 and TG9 $n$ = 4). Tukey post hoc revealed a significant weight reduction in the TG5 compared to WT at 6 months of age. B) Representative images of coronal OB sections with Nissl staining of BACHD rats and WT controls at 12 months of age are shown. Scale bar: 0.5 mm. C) The average area of the MCL + IPL + GCL is decreased in the TG5 and TG9 compared to WT at 12 months of age. Furthermore, the EPL averaged area is lower in TG5 rats compared to WT and TG9 (two-way ANOVA, Interaction p = 0.004; Genotype, p < 0.0001; Layers, p < 0.0001, WT, n = 4; TG5, $n$ = 5; TG9, n = 4). Tukey post hoc are presented on the graph. IPL = Internal plexiform layer, GCL = Granule cell layer, EPL = External plexiform layer, MCL = Mitral cell layer, GL = Glomerular layer. Error bar: SEM, post hoc between genotypes are presented on the graph.

the absence of variation detected in caspase-8 mRNA expression, a significant increase in the caspase-8 proform and p18 active fragment was observed at 3 months of age in the TG9 OB compared to WT (Proform: ANOVA p = 0.013, post hoc: WT vs. TG9, p < 0.05; p18: ANOVA p = 0.003, post hoc: WT vs. TG9, p < 0.01; TG5 vs. TG9, p < 0.05, Fig. 6G, Sup. Fig. 3), and a trend increase was also observed with the p43/41 fragments (p43/41: ANOVA p = 0.08, Fig. 6G, Sup. Fig. 3). Although no difference in the percent of active caspase-8 was detected between genotypes, a trend increase in the percentage of active caspase-8 was detected in 3-month-old TG9 OB compared to WT and TG5 OB (t-test, p < 0.05, Sup. Fig. 4). There was no further variation in caspase-3, -6 and -8 expression levels at 6 and 12 months of age (Fig. 6B-C, E-F, H-I, Sup. Fig. 3). In contrast to all the other caspases assessed, a significant increase in caspase-9 proform protein expression levels was observed only at the late time point (12 months of age) in the TG5 OB compared to WT (ANOVA p = 0.003, post hoc: WT vs. TG5, p < 0.05, Fig. 6J-L, Sup. Fig. 3). No cleaved fragments of caspase-9 were detected. In light of the alterations observed in the caspase expression profiles, we performed a TUNEL analysis of the OB at 12 months of age. We detected an increase in TUNEL-positive cells in the TG9 OB only, suggesting activation of the programmed cell death pathway is occurring in the TG9 line (Sup. Fig. 5, ANOVA Interaction, p = 0.04: Genotype, p = 0.08: Layers, p < 0.045). The increased number of TUNEL-positive cells are observed in the internal layers of the TG9 OB compared to WT and TG5 (post hoc: WT vs. TG9, p < 0.05; TG5 vs. TG9, p < 0.05).

## 4. Discussion

Assessment of olfactory dysfunction is described as a promising diagnostic marker for Mild Cognitive Impairment, Alzheimer's disease and Parkinson's disease, and may provide a sensitive measure of the early disease process in HD (Bahar-Fuchs et al., 2011; Barresi et al., 2012; Christen-Zaech et al., 2003; Delmaire et al., 2012; Djordjevic et al., 2008; Doty, 2012b; Mitchell et al., 2005; Moberg et al., 1987). Furthermore, in early grade human HD brain, there is a significant correlation between olfactory function and volume reduction of brain regions related to olfaction (Barrios et al., 2007). It therefore becomes important to determine the underlying mechanisms of the olfactory dysfunction in HD. As programmed cell death is an integral part of normal OB development and neuronal precursor evolution (Cowan and Roskams, 2004; Mori, 2014; Yan et al., 2001), and caspase activation has been shown to be an underlying mechanism in the striatal and cortical pathology in HD (Graham et al., 2006a; Ona et al., 1999; Rigamonti et al., 2001; Uribe et al., 2012; Wellington et al., 2002a; Wong et al., 2015), we assessed OB morphology and expression profiles of caspases and HTT in the BACHD rats. We demonstrate that there is atrophy of the OB in the TG5 and TG9 lines at specific time points and in specific layers of the OB. We also show enhanced cell death, and alterations in caspases protein expression profiles in the HD rat models

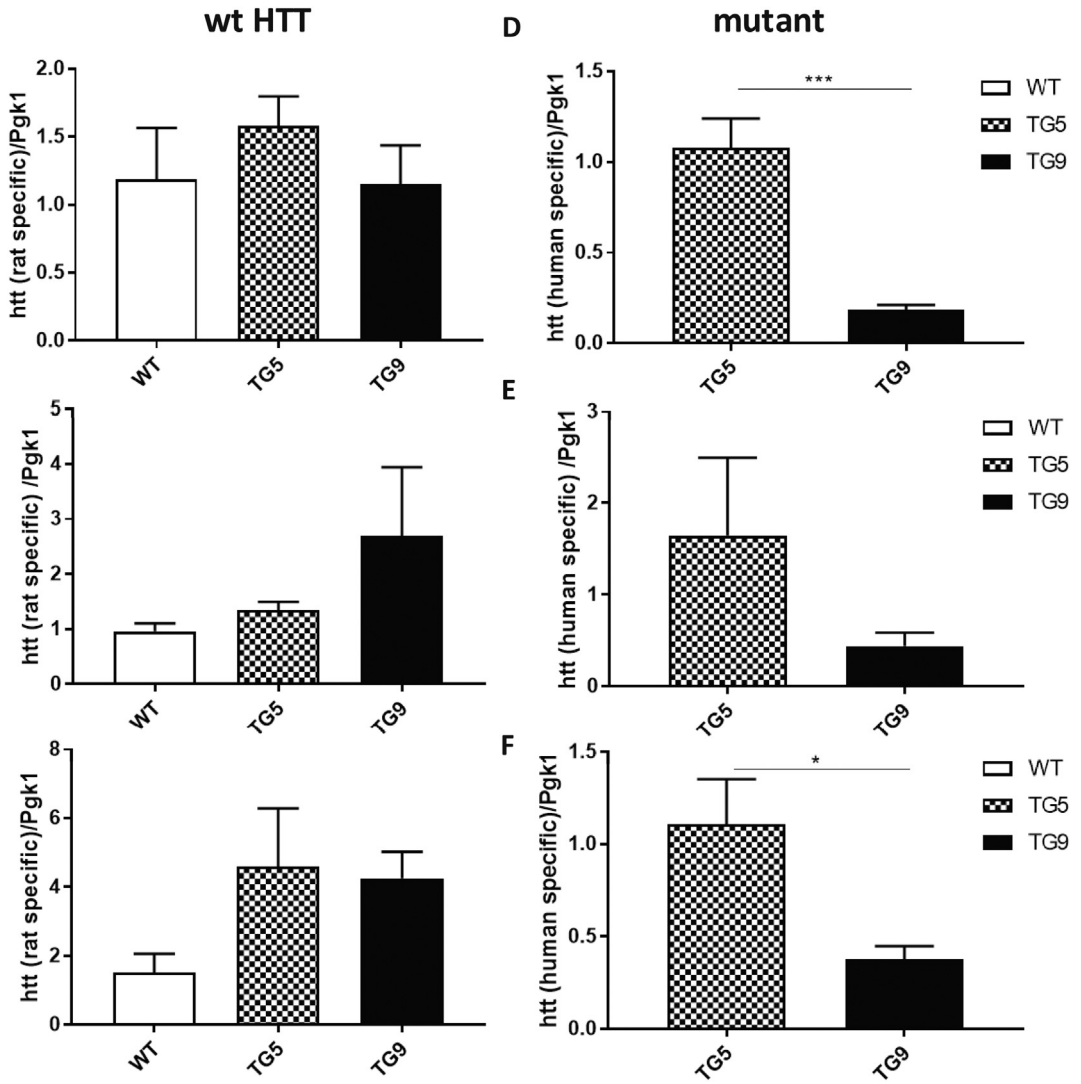


**Fig. 2.** Increased expression of mHTT mRNA in TG5 olfactory bulb compared to TG9 rats. A,B,C) No difference in endogenous HTT mRNA levels were observed at any age. However, a trend increase in TG9 vs. WT was observed at 12 months of age (t-test, $p < 0.05$). Increased mRNA expression of mHTT is observed in the OB of the TG5 line compared to TG9 at D) 3 ($p < 0.001$) and F) 12 months of age ($p < 0.05$). 3 months: WT $n = 4$, TG5 $n = 6$ and TG9 $n = 5$; 6 months: WT n = 4, TG5 $n = 3$ and TG9 n = 3; 12 months: WT n = 6, TG5 n = 4 and TG9 n = 6, relative measurements of HTT/pgk1 are ± SEM.

that do not correlate with their respective mRNA expression patterns (Table 1).

While the presence of olfactory impairment is widely observed in human HD, only limited studies on olfactory behaviour have been done in models of HD. Impaired olfactory sensitivity and odor discrimination has been observed in the R6/1 (Mo et al., 2014; Mo et al., 2015) and HdhQ111/+ HD mice respectively (Holter et al., 2013). As the morphology of several olfactory-related brain regions correlate with levels of olfactory function (Barrios et al., 2007; Buschhuter et al., 2008; Hummel et al., 2011), we analyzed the OB in the BACHD lines. Our results show a significant decrease in OB weight in the TG5 line, and a trend decrease in the TG9 rats, by 6 months of age. Further analysis of the area of the OB layers at 12 months of age shows that both lines display atrophy of the mitral cell, internal plexiform and granule cell layers, while atrophy of the external plexiform is only significant in the TG5 line. These results are concordant with previous studies demonstrating that OB atrophy is a common event in neurodegenerative diseases which display signs of olfactory dysfunction (Brodoehl et al., 2012; Chen et al., 2014; Servello et al., 2015; ter Laak et al., 1994; Thomann et al., 2009; Wang et al., 2011) and in HD murine models (Carroll et al., 2011; Smail et al., 2016) (Carroll et al., 2011; Smail et al., 2016). As alterations in the development of the mitral cell layer can affect odor discrimination (Bastakis et al., 2015), the atrophy of the internal layers (MCL, IPL and GCL) observed here could be involved in the olfaction impairment observed in HD. Furthermore, an increase in apoptosis of granule cells may be an important process for the olfactory information processing by eliminating the specific Granule cells and therefore reducing the signal-to-noise ratio which may help the olfactory learning and memory (Yamaguchi et al., 2013). The internal layers contain a population of immature cells. It is therefore possible that the decrease in the internal layers of the OB in the BACHD lines could also reflect a neurogenesis impairment previously observed in HD (Curtis et al., 2003; Fedele et al., 2011; Kohl et al., 2010; Phillips et al., 2005; Simpson et al., 2011). Indeed, we observed a trend decrease in OB NeuN (marker of mature neurons) protein expression at 6 months of age in both lines indicating that neurogenesis may be impaired.

Significant evidence in the literature supports a mHTT dose-dependent neurodegenerative effect (de Almeida et al., 2002; Graham et al., 2006b; Hodgson et al., 1999; Reddy et al., 1998; Squitieri et al., 2003). This has also been demonstrated in the BACHD models with the TG5 line showing higher mHTT expression overall (this study and Yu-Taeger et al., 2012) and earlier motor deficits compared to the TG9 line

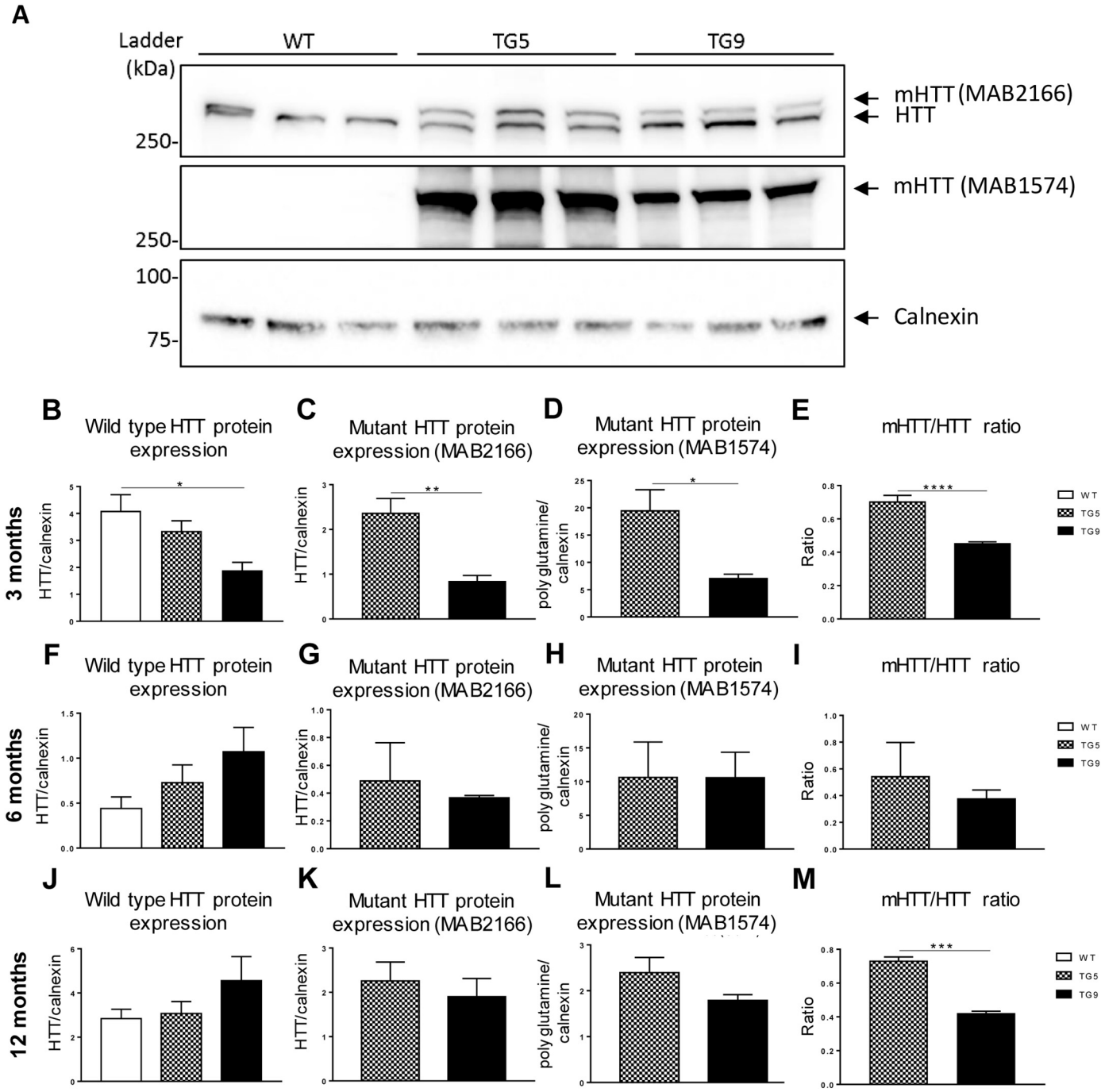


**Fig. 3.** Age-specific alterations in the protein expression of HTT in TG5 and TG9 olfactory bulb. A) Representative images of western blots for HTT and mHTT obtained with MAB2166 (first panel) and MAB1574 (second panel) antibodies on 12-month old OB lysates. The reference protein used is calnexin. B) At 3 months of age, decreased expression of wild type HTT is observed in the TG9 OB compared to WT (ANOVA $p = 0.016$, post hoc WT vs. TG9, $p < 0.05$). A higher expression of mHTT is observed by western blot in TG5 compared to TG9 OB when using C) MAB2166 (t-test, $p < .01$) and D) MAB1574 (t-test, $p < 0.05$) antibodies. E) A lower mHTT/HTT ratio is observed in TG9 when compared to TG5 (t-test, $p < 0.0001$, MAB2166). F—I) No significant variation in the expression of endogenous or mHTT is observed between genotypes at 6 months of age. J-L) At 12 months of age, no variation was detected in the wild type HTT or mHTT protein expression between genotypes. M) A lower mHTT/HTT ratio is observed in TG9 OB when compared to TG5 (t-test, $p < 0.001$, MAB2166) at 12 months of age. Mean measurements and densitometric ratios of mHTT/endogenous HTT are ± SEM, $n = 6$ for all genotypes at 3 months of age and $n = 3$ for all genotypes at 6 and 12 months of age. MAB2166: Anti-huntingtin, MAB1574: Anti-Polyglutamine-Expansion disease marker.

(Yu-Taeger et al., 2012). Furthermore, mHTT gradually affects the volume of several brain regions (Aylward et al., 1994; Aylward et al., 1996). The same gradual decrease was observed in the OB weight of TG5 rats. In the TG9 line, which expresses less mHTT in the OB overall than the TG5 line, there is also atrophy but less than in TG5 (albeit the difference is subtle).

The expression of several caspases is deregulated in HD and active fragments of caspases are found in postmortem HD brains (Graham et al., 2010; Kiechle et al., 2002; Kim et al., 2001; Wanker, 2002; Wellington et al., 2002a). This deregulation in caspase activation could lead to not only cell death but also alterations in neurogenesis and development of the OB. Indeed, half of the newborn interneurons are

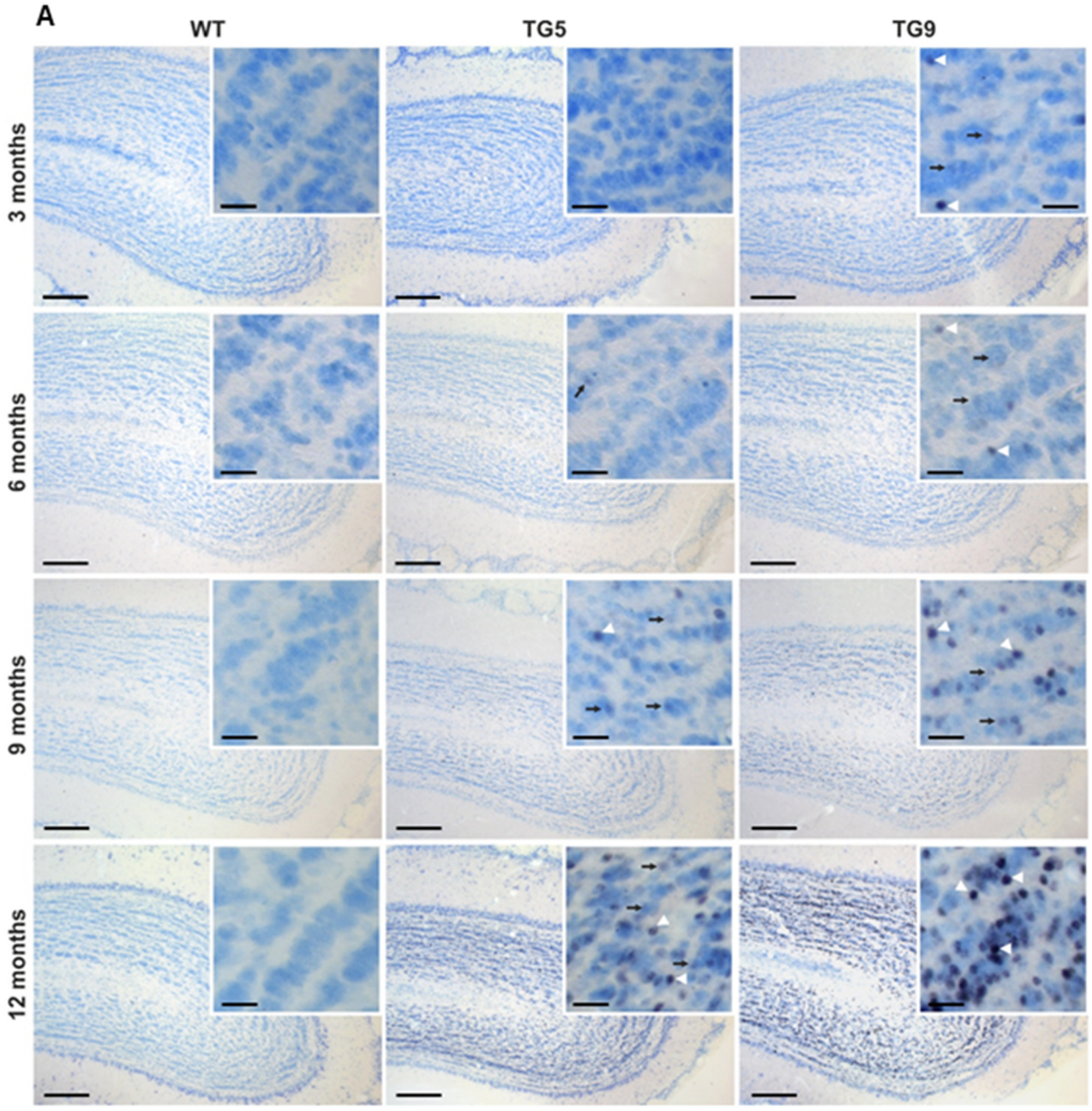


(caption on next page)

**Fig. 4.** Prominent nuclear accumulation of mHTT in BACHD TG9 rats. A) Nuclear accumulation of mHTT was investigated by immunohistochemistry using the antibody S830 against HTT (black color) in the OB of BACHD lines TG5 and TG9 at 3, 6, 9 and 12 months of age. Sections were counterstained with thionine to visualize nuclei (blue color). Transgenic rats of TG9 exhibit condensed nuclear accumulation (arrow heads) starting at 3 months of age which dramatically increase with age, while transgenic rats of TG5 show only a weak nuclear staining (arrows) by S830 stating at 6 months of age. Until 12 months of age the immunoreactivity of anti-HTT S830 antibody is more intense in rats of the TG9 line compared to rats of TG5. WT littermates serve as negative controls and show no positive signal for mHTT in all time points investigated. Scale bar = 20 and 200 um. B) The quantification of the nuclear accumulation of mHTT in TG5 compared to TG9 demonstrates there is an interaction between the genotype ($p < 0.0001$), an effect of the age ($p < 0.0001$), and an effect of the genotype ($p < 0.0001$) by two-way ANOVA. Sidak's post hoc are presented in the graph. Results are presented ± SEM. (For interpretation of the references to color in this figure legend, the reader is referred to the web version of this article.)

eliminated by apoptosis before their incorporation into specific locations in the OB (Mori, 2014). The analysis of OB caspases expression profiles in the TG5 and TG9 HD rat models shows an increase or a trend increase in cleavage fragments of caspase-3 and -8 in TG9, implying the activation of these caspases by 3 months of age. This increase in active caspase fragments may explain the atrophy observed later. At older ages, increases in caspase-3 mRNA was also observed in this line. However, this did not translate into increases at the protein level at those time-points. In our results, the caspase protein expression data does not follow the same trend as the mRNA levels. Changes in mRNA may be buffered by translational changes or post-translational modifications of the protein as previously shown (Ishikawa et al., 2017; Perl et al., 2017). Furthermore, although the activation of caspase-3 has previously been observed in human HD striatum (Graham et al., 2010; Kim et al., 2001) and indeed used as a routine marker of cell death (Chen et al., 2015; Karamitopoulou et al., 2007; Mazumder et al., 2008), it is not clear whether the activation of caspase-3 observed in our results reflects impending cell death or issues with neurodevelopment. It has been previously demonstrated that the presence of caspase-3 affects the structural development of the OB as a deficiency in murine caspase-3 leads to abnormal development of the OB (Cowan and Roskams, 2004).

Similar to our results, an increase in caspase-8 has been previously reported in human HD caudate and caspase-8 shown to be required in cell death pathways caused by an expanded polyglutamine disease (Sanchez et al., 1999a). In contrast to the other caspases, a decrease in the proform and the p20p10 fragment of caspase-6 is observed in the OB of the BACHD lines. The p20p10 fragment is not an active fragment per se, rather it is an intermediate fragment of caspase-6, lacking the pro-domain, that has been shown to be required for the activation of caspase-6 and is further cleaved into the activated form (Klaiman et al., 2009). It is important to point out that some in vivo caspase active fragments, such as for caspase-6, are difficult to visualize by Western Blot (Warby et al., 2008). Therefore, we cannot rule out the possibility that the increase in caspase-6 gene expression, combined with the decrease in the proform and p20p10 fragment of caspase-6, may reflect the activation of caspase-6. This is concordant with the caspase-6 activation observed in the striatum and cortex of human and murine HD brain (Graham et al., 2010; Hermel et al., 2004b).

The activation of caspases observed in TG9 does correlates with the atrophy observed in this line. However, as cell death is an important part of the development of the OB and neurogenesis, the activation of the caspases observed predominantly at 3 months of age may also reflect an impairment in development that is occurring at that age which then persists. This is supported by the observation that in the WT OBs, there is a 21% increase in OB weight between 3 and 6 months of age which is not found in the BACHD OBs (TG5: −14% and TG9: −8%). An impairment in proliferation pathways may cause the decreases in OB weight and trend decrease in the NeuN expression at 6 months of age. It is also possible that the area of the cell may shrink in the presence of mHTT leading to the decrease in OB weight, as previously observed in an HD striatal cell line and human HD cortex (Rajkowska et al., 1998; Singer et al., 2017).

Our results do show that there is increased TUNEL positive cells, and therefore cell death, at the 12 month time point in the TG9 OB which correlates with the increases in caspase-3 mRNA and atrophy observed. However, we do not see changes in the other caspases assessed at this time point. It is possible that these changes may have occurred prior, and/or different caspases may be implicated. Furthermore, it is possible that the variation in caspases expression is not uniform throughout the OB and is only observed in specific layers of the bulb, as suggested by the absence of atrophy in the glomerular layer. As the entire OB was used for the caspase expression analysis, this may have diluted any specific effects. It is also important to mention that the alterations observed in caspase expression in our results may reflect not only the death of OB cells in general, but also affect the cellular composition of the OB and therefore ultimately olfactory function.

In our results, the immunostaining of mHTT (using S830 antibody), which has been reported to correlate with disease progression (Acton, 2013), shows early and substantially more nuclear accumulation of mHTT in the internal layers of TG9 OBs compared to TG5. As some N-terminal fragments of HTT interact with the Trp protein and decrease the nuclear export of HTT (Cornett et al., 2005), the difference in the nuclear accumulation of HTT in the BACHD lines may be caused by an increased production of the caspase generated N-terminal fragments of HTT in the TG9 OBs. This correlates with the decrease in full length HTT and caspase-3 activation observed in this line. As wild type HTT has been shown to inhibit caspase-3 activation (Zhang et al., 2006), it is possible that the decrease in wild type HTT observed may have affected its inhibitory affect on caspase-3 thus influencing its activation. As mHTT aggregates can interact with transcription factor via their polyglutamine sequence (Boutell et al., 1999; Li et al., 2016; Shimohata et al., 2000; Steffan et al., 2000), mHTT accumulation in the TG9 line may alter the transcription process and lead to the increased cell death observed by TUNEL. Moreover, it has been shown that caspase-3, -8, -10 and -12, (in contrast to caspase-9) interact and are activated by expanded polyglutamine motifs (Gervais et al., 2002; Kouroku et al., 2002; Kouroku et al., 2000; Miyashita et al., 1999; Sanchez et al., 1999a; U et al., 2001). Of note, the interaction with caspase-8 occurs predominantly in the nuclear aggregates containing fragments of polyQ repeats (U et al., 2001). The increased accumulation of mHTT in the nucleus, along with the activation of casapse-3, -6 and -8, in the TG9 line and absence of any caspase-9 proteolytic fragments, may contribute to the atrophy observed in the TG9 OB and cell death observed by TUNEL.

A key question is why caspase-3 and -8 activation are only observed in the TG9 line. This is not due to differences in the transgene or the CAG size (Yu-Taeger et al., 2012). One reason may be related to the increased mHTT accumulation as the accumulation of misfolded protein impairs cell function (Vilchez et al., 2014). Another reason may be the spatial and temporal expression pattern of HTT and mHTT in these lines. A study has shown that the chromosomal location of a transgenes can create disparities in the molecular phenotypes between lines created with the same transgene and can affect the expression of the transgene in an organ-related manner (Hatada et al., 1999). Therefore, the differential expression and activation of caspases may be due to the insertion site of the HD gene in these models. Similar to the increase observed at the mRNA and protein level in our results, it has previously been shown that the TG5 line expresses overall more mHTT (Yu-Taeger et al., 2012). It is possible that some enhancers near the insertion site alter the expression of mHTT in the TG5 line in some brain regions. A

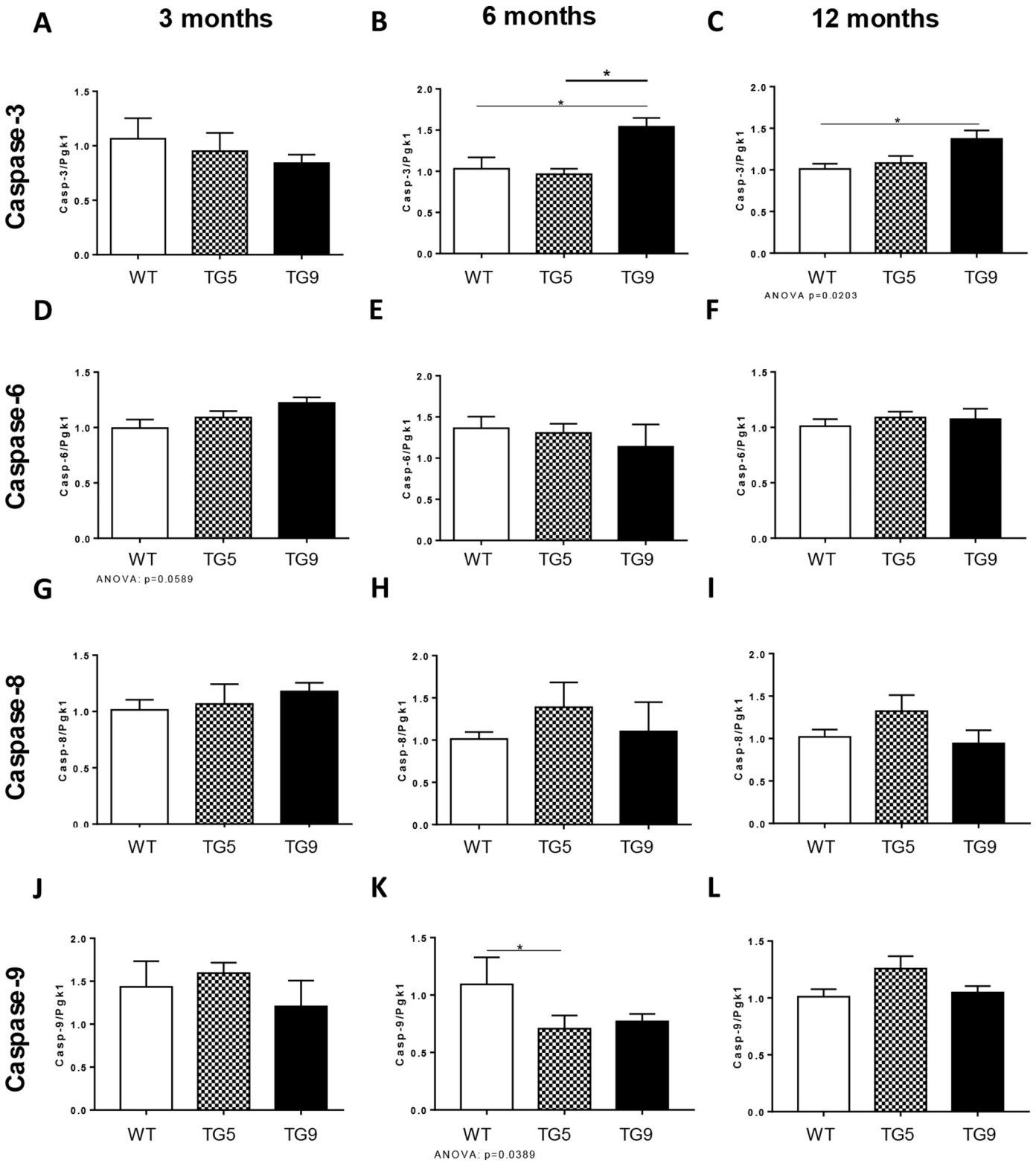


**Fig. 5.** Variations in caspase mRNA expression profiles in the olfactory bulb of BACHD models. A-C) Real-time quantitative RT-PCR shows an increase in caspase-3 mRNA expression levels in TG9 OB at 6 and 12 months of age compared to WT (6 months: ANOVA $p = 0.03$, post hoc: WT vs TG9 $p < 0.05$; 12 months: ANOVA $p = 0.02$, post hoc: WT vs TG9 $p < 0.05$). D-F) A trend increase in OB caspase-6 mRNA expression levels is observed at 3 months of age in TG9 vs. WT (ANOVA $p = 0.059$, t-test: WT vs TG9 $p < 0.05$). G-I) No variation in caspase-8 mRNA expression levels is detected in TG5 and TG9 OB compared to WT at any age assessed. J-L) A decrease is observed in caspase-9 mRNA expression levels in TG5 at 6 months of age and a trend decrease observed at 3 months of age in TG9 OB compared to WT (3 months: ANOVA $p = 0.08$, t-test: WT vs TG9, $p < 0.05$; 6 months: ANOVA $p = 0.04$, post hoc, WT vs. TG5, $p < 0.05$). 3 months: WT $n = 6$, TG5 n = 6 and TG9 n = 6; 6 months: WT $n = 4$, TG5 $n = 3$ and TG9 n = 3 12 months: WT n = 6, TG5 n = 4 and TG9 n = 6; Dunnet post hoc are presented on graph. Pgk1 used as reference control. Relative measurements of caspase/pgk1 are ± SEM.

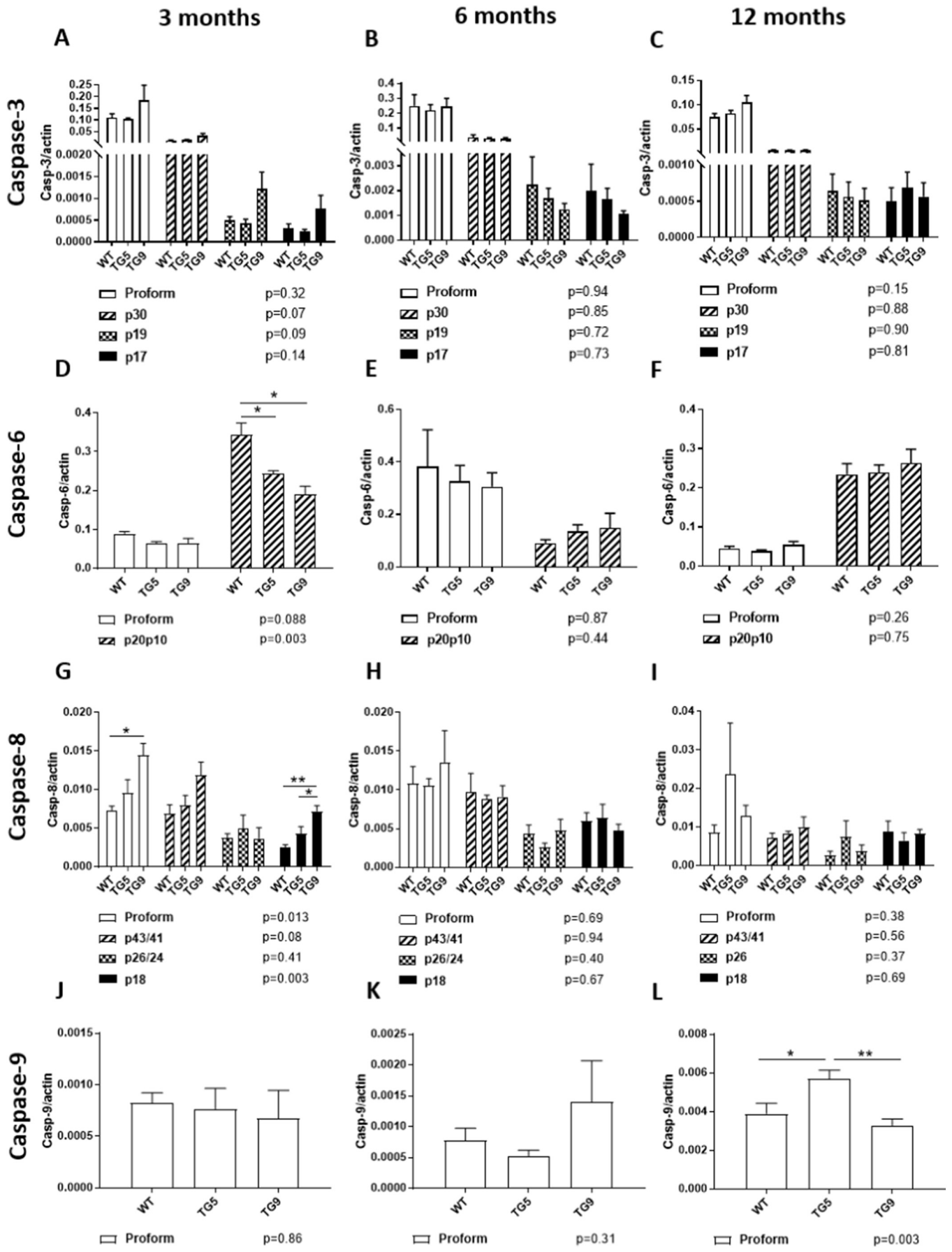


*(caption on next page)*

**Fig. 6.** Early changes in caspase protein expression in the olfactory bulb of BACHD rats. A-C) A tendency to an increase in caspase-3 active fragment is observed at 3 months of age in TG9 OB, no further variation is observed at a later time point (p30: ANOVA p = 0.07; p19: ANOVA p = 0.09). D-F) A decrease, or a trend decrease in caspase-6 proform and p20p10 expression levels is observed at 3 months of age in TG5 and TG9 compared to WT OB (Proform: ANOVA p = 0.09, t-test: WT vs. TG5 p < 0.05; p20p10: ANOVA p = 0.003, post hoc: WT vs. TG5, p < 0.05; WT vs. TG9, p < 0.05) G-I) Increased expression of the caspase-8 proform, p43/41 and p18 fragments are detected in TG9 OB when compared to WT at 3 months of age (Proform: ANOVA p = 0.013, post hoc: WT vs. TG9, p < 0.05; p43/41: ANOVA p = 0.08, t-test: WT vs. TG9 $p = .052$; p18: ANOVA p = 0.003, post hoc: WT vs. TG9, p < 0.01; TG5 vs. TG9, p < 0.05) J-L) In sharp contrast to the other caspases, an increase in caspase-9 proform is observed only at 12 months of age in TG5 OB compared to WT (ANOVA p = 0.003, post hoc: WT vs. TG5, p < 0.05). The reference protein used is actin. The *p* values of the one-way ANOVA are presented below the graph for each form. Mean measurements and densitometric ratios of caspases/actin are ± SEM, 3 months: WT $n = 4$ for all genotypes; 6 months: WT n = 4, TG5 $n = 3$ and TG9 n = 3; 12 months: WT $n = 6$, TG5 n = 6 and TG9 $n = 7$.

**Table 1**
Summary of huntingtin and caspase expression profiles in TG5 and TG9 BACHD OB compared to WT.

| | | 3 months vs WT | | 6 months vs WT | | 12 months vs WT | |
|---|---|---|---|---|---|---|---|
| | | TG5 | TG9 | TG5 | TG9 | TG5 | TG9 |
| Huntingtin | mRNA - wt htt | – | – | – | – | – | ↑ |
| | mRNA - mhtt | ↑ vs TG9 | ↓ vs TG5 | – | – | ↑ vs TG9 | ↓ vs TG5 |
| | wild type htt | – | ↓ | – | – | – | – |
| | mhtt (MAB2166) | ↑ vs TG9 | ↓ vs TG5 | – | – | – | – |
| | mhtt (MAB1574) | ↑ vs TG9 | ↓ vs TG5 | – | – | – | – |
| | Ratio mhtt/htt | ↑ vs TG9 | ↓ vs TG5 | – | – | ↑ vs TG9 | ↓ vs TG5 |
| | Nuclear htt accumulation | – | ↑ | ↑ | ↑↑ | ↑↑ | ↑↑↑ |
| Caspase 3 | mRNA | – | – | – | ↑ | – | ↑ |
| | Proform | – | – | – | – | – | – |
| | p30 | – | ↑ | – | – | – | – |
| | p19 | – | ↑ | – | – | – | – |
| | p17 | – | – | – | – | – | – |
| | % active caspase | – | ↑ vs TG5 | – | – | – | – |
| Caspase 6 | mRNA | – | ↑ | – | – | – | – |
| | Proform | ↓ | – | – | – | – | – |
| | p20p10 | ↓ | ↓ | – | – | – | – |
| | % active caspase | – | – | – | – | – | – |
| Caspase 8 | mRNA | – | – | – | – | – | – |
| | Proform | – | ↑ | – | – | – | – |
| | p43/41 | – | ↑ | – | – | – | – |
| | p26/24 | – | – | – | – | – | – |
| | p18 | – | ↑ | – | – | – | – |
| | % active caspase | – | ↑ | – | – | – | – |
| Caspase 9 | mRNA | – | ↓ | ↓ | – | – | – |
| | Proform | – | – | – | – | ↑ | – |
| Cell death | TUNEL-positive cells | ND | ND | ND | ND | – | ↑ |

Caspase-3: p30 = 30 kDa fragment, p19 = 19 kDa fragment, p17 = 17 kDa fragment, Caspase-6: p20p10 = CASP6 without the prodomain, Caspase-8: p43/41 = 43 and 41 kDa fragments, p26/24 = 26 and 24 kDa fragments, p18 = 18 kDa fragment. Proform = full-length form of the caspase protein. The sign « – » represents no significant variation between the BACHD rat model and the WT. ND = Not Done.

difference in the spatial distribution of mHTT in TG5 vs. TG9 lines may explain the discrepancy observed in the behaviour and brain pathology between them. Indeed, in addition to the differences observed in this study (lack of caspase-3 and -8 activation in the TG5 OB and reduced OB mHTT nuclear accumulation compared to TG9) the TG5 line displays earlier motor deficits (accelerated rotarod, gait analysis) and decreased rearing activities compared to TG9. However, both lines display similar deficits in ambulatory activities, reduced food intake and HD gene expression signatures of a similar magnitude (Yu-Taeger et al., 2017; Yu-Taeger et al., 2012). These results highlight the necessity of comparing different lines and strains in animal models.

## 5. Conclusion

Our results show a significant decrease in the OB at specific time points in the BACHD transgenic lines. The atrophy is predominantly detected in the internal layers of the OB while the glomerular layer area is not affected. Furthermore, variations in caspase mRNA expression levels, and alterations in caspase protein expression levels are observed. We also detected a differential expression and localization profile of normal and mutant HTT in TG5 compared to the TG9 line. Despite the increase in mHTT expression in the TG5 OBs, TG9 rats demonstrate caspase-3 and -8 activation in the OB,more accumulation of HTT in the nucleus and more cell death. These data provide important information regarding the olfactory dysfunction observed in HD and further implicate alterations in apoptosis and neurogenesis as underlying mechanisms in the pathogenesis of HD.

## Acknowledgements

This research was undertaken with a research grant from the Huntington Society of Canada, Research Centre on Aging, and, in part, by the Canada Research chairs program. Support was also provided by the European Union 7th Framework Program (FP7/2012), Project “SWITCH-HD”, under grant agreement No. 324495 to H.P.N. RKG holds the Canada Research Chair in Neurodegenerative diseases.

## Appendix A. Supplementary data

Supplementary data to this article can be found online at https://doi.org/10.1016/j.nbd.2019.02.002.

## References

Abada, Y.S., et al., 2013. Motor, emotional and cognitive deficits in adult BACHD mice: a model for Huntington's disease. Behav. Brain Res. 238, 243–251.
Acton, Q.A., 2013. Huntington's Disease: New Insights for the Healthcare Professional. ScholarlyEditions, Atlanta, Georgia.
Aylward, E.H., et al., 1994. Reduced basal ganglia volume associated with the gene for

Huntington's disease in asymptomatic at-risk persons. Neurology 44, 823–828.
Aylward, E.H., et al., 1996. Basal ganglia volume and proximity to onset in presymptomatic Huntington disease. Arch. Neurol. 53, 1293–1296.
Bacon Moore, A.S., et al., 1999. A test of odor fluency in patients with Alzheimer's and Huntington's disease. J. Clin. Exp. Neuropsychol. 21, 341–351.
Bahar-Fuchs, A., et al., 2011. Awareness of olfactory deficits in healthy aging, amnestic mild cognitive impairment and Alzheimer's disease. Int. Psychogeriatr. 23, 1097–1106.
Barresi, M., et al., 2012. Evaluation of olfactory dysfunction in neurodegenerative diseases. J. Neurol. Sci. 323, 16–24.
Barrios, F.A., et al., 2007. Olfaction and neurodegeneration in HD. Neuroreport 18, 73–76.
Bastakis, G.G., et al., 2015. Tag1 deficiency results in olfactory dysfunction through impaired migration of mitral cells. Development 142, 4318–4328.
Boutell, J.M., et al., 1999. Aberrant interactions of transcriptional repressor proteins with the Huntington's disease gene product, huntingtin. Hum. Mol. Genet. 8, 1647–1655.
Brodoehl, S., et al., 2012. Decreased olfactory bulb volume in idiopathic Parkinson's disease detected by 3.0-tesla magnetic resonance imaging. Mov. Disord. 27, 1019–1025.
Burns, A., et al., 1990. Clinical assessment of irritability, aggression, and apathy in Huntington and Alzheimer disease. J. Nerv. Ment. Dis. 178, 20–26.
Buschhuter, D., et al., 2008. Correlation between olfactory bulb volume and olfactory function. NeuroImage 42, 498–502.
Bylsma, F.W., et al., 1997. Odor identification in Huntington's disease patients and asymptomatic gene carriers. J. Neuropsychiatry Clin. Neurosci. 9, 598–600.
Carroll, J.B., et al., 2011. Natural history of disease in the YAC128 mouse reveals a discrete signature of pathology in Huntington disease. Neurobiol. Dis. 43, 257–265.
Cattaneo, E., et al., 2005. Normal huntingtin function: an alternative approach to Huntington's disease. Nat. Rev. Neurosci. 6, 919–930.
Chen, S., et al., 2014. Imaging of olfactory bulb and gray matter volumes in brain areas associated with olfactory function in patients with Parkinson's disease and multiple system atrophy. Eur. J. Radiol. 83, 564–570.
Chen, D.L., et al., 2015. Imaging caspase-3 activation as a marker of apoptosis-targeted treatment response in cancer. Mol. Imaging Biol. 17, 384–393.
Christen-Zaech, S., et al., 2003. Early olfactory involvement in Alzheimer's disease. Can. J. Neurol. Sci. 30, 20–25.
Cornett, J., et al., 2005. Polyglutamine expansion of huntingtin impairs its nuclear export. Nat. Genet. 37, 198–204.
Cowan, C.M., Roskams, A.J., 2004. Caspase-3 and caspase-9 mediate developmental apoptosis in the mouse olfactory system. J. Comp. Neurol. 474, 136–148.
Cummings, J.L., 1995. Behavioral and psychiatric symptoms associated with Huntington's disease. Adv. Neurol. 65, 179–186.
Curtis, M.A., et al., 2003. Increased cell proliferation and neurogenesis in the adult human Huntington's disease brain. Proc. Natl. Acad. Sci. U. S. A. 100, 9023–9027.
Curtis, M.A., et al., 2005. The distribution of progenitor cells in the subependymal layer of the lateral ventricle in the normal and Huntington's disease human brain. Neuroscience 132, 777–788.
de Almeida, L.P., et al., 2002. Lentiviral-mediated delivery of mutant huntingtin in the striatum of rats induces a selective neuropathology modulated by polyglutamine repeat size, huntingtin expression levels, and protein length. J. Neurosci. 22, 3473–3483.
Delmaire, C., et al., 2012. The structural correlates of functional deficits in early huntington's disease. Hum. Brain Mapp. 34, 2141–2153.
Djordjevic, J., et al., 2008. Olfaction in patients with mild cognitive impairment and Alzheimer's disease. Neurobiol. Aging 29, 693–706.
Doty, R.L., 2012a. Olfaction in Parkinson's disease and related disorders. Neurobiol. Dis. 46, 527–552.
Doty, R.L., 2012b. Olfactory dysfunction in Parkinson disease. Nat. Rev. Neurol. 8, 329–339.
Fedele, V., et al., 2011. Neurogenesis in the R6/2 mouse model of Huntington's disease is impaired at the level of NeuroD1. Neuroscience 173, 76–81.
Ferris, C.F., et al., 2014. Studies on the Q175 Knock-in Model of Huntington's Disease using Functional Imaging in Awake mice: evidence of Olfactory Dysfunction. Front. Neurol. 5, 94.
Gafni, J., et al., 2004. Inhibition of calpain cleavage of huntingtin reduces toxicity: accumulation of calpain/caspase fragments in the nucleus. J. Biol. Chem. 279, 20211–20220.
Gervais, F.G., et al., 2002. Recruitment and activation of caspase-8 by the Huntingtin-interacting protein Hip-1 and a novel partner Hippi. Nat. Cell Biol. 4, 95–105.
Goldberg, Y.P., et al., 1996. Cleavage of huntingtin by apopain, a proapoptotic cysteine protease, is modulated by the polyglutamine tract. Nat. Genet. 13, 442–449.
Graham, R.K., et al., 2006a. Cleavage at the caspase-6 site is required for neuronal dysfunction and degeneration due to mutant huntingtin. Cell 125, 1179–1191.
Graham, R.K., et al., 2006b. Levels of mutant huntingtin influence the phenotypic severity of Huntington disease in YAC128 mouse models. Neurobiol. Dis. 21, 444–455.
Graham, R.K., et al., 2010. Cleavage at the 586 amino acid caspase-6 site in mutant huntingtin influences caspase-6 activation in vivo. J. Neurosci. 30, 15019–15029.
Graham, R.K., et al., 2012. Caspase-6-resistant mutant Huntingtin does not rescue the toxic effects of Caspase-Cleavable Mutant Huntingtin in vivo. J. Huntingtons Dis. 1, 243–260.
Hamilton, J.M., et al., 1999. Odor detection, learning, and memory in Huntington's disease. J. Int. Neuropsychol. Soc. 5, 609–615.
Han, M.H., et al., 2016. Current opinion on the role of neurogenesis in the therapeutic strategies for Alzheimer Disease, Parkinson Disease, and Ischemic Stroke; considering neuronal voiding function. Int. Neurourol. J. 20, 276–287.
Hatada, S., et al., 1999. The influence of chromosomal location on the expression of two transgenes in mice. J. Biol. Chem. 274, 948–955.
Hermel, E., et al., 2004a. Specific caspase interactions and amplification are involved in selective neuronal vulnerability in Huntington's disease. Cell Death Differ. 11, 424–438.
Hermel, E., et al., 2004b. Specific caspase interactions and amplification are involved in selective neuronal vulnerability in Huntington's disease. Cell Death Differ. 11, 424–438.
Hodgson, J.G., et al., 1999. A YAC mouse model for Huntington's disease with full-length mutant huntingtin, cytoplasmic toxicity, and selective striatal neurodegeneration. Neuron 23, 181–192.
Holter, S.M., et al., 2013. A broad phenotypic screen identifies novel phenotypes driven by a single mutant allele in Huntington's disease CAG knock-in mice. PLoS One 8, e80923.
Hummel, T., et al., 2011. Correlation between olfactory bulb volume and olfactory function in children and adolescents. Exp. Brain Res. 214, 285–291.
Ishikawa, K., et al., 2017. Post-translational dosage compensation buffers genetic perturbations to stoichiometry of protein complexes. PLoS Genet. 13, e1006554.
Jankovic, J., Roos, R.A., 2014. Chorea associated with Huntington's disease: to treat or not to treat? Mov. Disord. 29, 1414–1418.
Karamitopoulou, E., et al., 2007. Active caspase 3 and DNA fragmentation as markers for apoptotic cell death in primary and metastatic liver tumours. Pathology 39, 558–564.
Kiechle, T., et al., 2002. Cytochrome C and caspase-9 expression in Huntington's disease. NeuroMolecular Med. 1, 183–195.
Kim, Y.J., et al., 2001. Caspase 3-cleaved N-terminal fragments of wild-type and mutant huntingtin are present in normal and Huntington's disease brains, associate with membranes, and undergo calpain-dependent proteolysis. Proc. Natl. Acad. Sci. 98, 12784–12789.
Kim, M.J., et al., 2002. Calpain-dependent cleavage of cain/cabin1 activates calcineurin to mediate calcium-triggered cell death. Proc. Natl. Acad. Sci. U. S. A. 99, 9870–9875.
Klaiman, G., et al., 2009. Self-activation of Caspase-6 in vitro and in vivo: Caspase-6 activation does not induce cell death in HEK293T cells. Biochim. Biophys. Acta 1793, 592–601.
Kohl, Z., et al., 2010. Impaired adult olfactory bulb neurogenesis in the R6/2 mouse model of Huntington's disease. BMC Neurosci. 11 (114-2202-11-114).
Kouroku, Y., et al., 2000. Caspases that are activated during generation of nuclear polyglutamine aggregates are necessary for DNA fragmentation but not sufficient for cell death. J. Neurosci. Res. 62, 547–556.
Kouroku, Y., et al., 2002. Polyglutamine aggregates stimulate ER stress signals and caspase-12 activation. Hum. Mol. Genet. 11, 1505–1515.
Larsson, M., et al., 2006. Olfactory functions in asymptomatic carriers of the Huntington disease mutation. J. Clin. Exp. Neuropsychol. 28, 1373–1380.
Lazic, S.E., et al., 2007. Olfactory abnormalities in Huntington's disease: decreased plasticity in the primary olfactory cortex of R6/1 transgenic mice and reduced olfactory discrimination in patients. Brain Res. 1151, 219–226.
Li, L., et al., 2016. Real-time imaging of Huntingtin aggregates diverting target search and gene transcription. elife 5.
Lunkes, A., et al., 2002. Proteases acting on mutant huntingtin generate cleaved products that differentially build up cytoplasmic and nuclear inclusions. Mol. Cell 10, 259–269.
Mazumder, S., et al., 2008. Caspase-3 activation is a critical determinant of genotoxic stress-induced apoptosis. Methods Mol. Biol. 414, 13–21.
Menalled, L.B., et al., 2003. Time course of early motor and neuropathological anomalies in a knock-in mouse model of Huntington's disease with 140 CAG repeats. J. Comp. Neurol. 465, 11–26.
Mende-Mueller, L.M., et al., 2001. Tissue-specific proteolysis of Huntingtin (htt) in human brain: evidence of enhanced levels of N- and C-terminal htt fragments in Huntington's disease striatum. J. Neurosci. 21, 1830–1837.
Metzler, M., et al., 2010. Phosphorylation of huntingtin at Ser421 in YAC128 neurons is associated with protection of YAC128 neurons from NMDA-mediated excitotoxicity and is modulated by PP1 and PP2A. J. Neurosci. 30, 14318–14329.
Milnerwood, A.J., et al., 2010. Early increase in extrasynaptic NMDA receptor signaling and expression contributes to phenotype onset in Huntington's disease mice. Neuron 65, 178–190.
Mitchell, I.J., et al., 2005. Huntington's disease patients show impaired perception of disgust in the gustatory and olfactory modalities. J. Neuropsychiatry Clin. Neurosci. 17, 119–121.
Miyashita, T., et al., 1999. Expression of extended polyglutamine sequentially activates initiator and effector caspases. Biochem. Biophys. Res. Commun. 257, 724–730.
Mo, C., et al., 2014. Effects of chronic stress on the onset and progression of Huntington's disease in transgenic mice. Neurobiol. Dis. 71, 81–94.
Mo, C., et al., 2015. Novel ethological endophenotypes in a transgenic mouse model of Huntington's disease. Behav. Brain Res. 276, 17–27.
Moberg, P.J., Doty, R.L., 1997. Olfactory function in Huntington's disease patients and at-risk offspring. Int J Neurosci. 89, 133–139.
Moberg, P.J., et al., 1987. Olfactory recognition: differential impairments in early and late Huntington's and Alzheimer's diseases. J. Clin. Exp. Neuropsychol. 9, 650–664.
Mori, K., 2014. The Olfactory System : From Odor Molecules to Motivational Behaviors. Springer, Tokyo; New York.
Mouret, A., et al., 2009. Turnover of newborn olfactory bulb neurons optimizes olfaction. J. Neurosci. 29, 12302–12314.
Nordin, S., et al., 1995. Sensory- and memory-mediated olfactory dysfunction in Huntington's disease. J. Int. Neuropsychol. Soc. 1, 281–290.
Ona, V.O., et al., 1999. Inhibition of caspase-1 slows disease progression in a mouse model of Huntington's disease. Nature 399, 263–267.
Paulsen, J.S., et al., 2008. Detection of Huntington's disease decades before diagnosis: the Predict-HD study. J. Neurol. Neurosurg. Psychiatry 79, 874–880.

Paulsen, J.S., et al., 2014. Clinical and biomarker changes in Premanifest Huntington Disease Show Trial Feasibility: a Decade of the PREDICT-HD Study. Front. Aging Neurosci. 6, 78.
Perl, K., et al., 2017. Reduced changes in protein compared to mRNA levels across non-proliferating tissues. BMC Genomics 18, 305.
Phillips, W., et al., 2005. Abnormalities of neurogenesis in the R6/2 mouse model of Huntington's disease are attributable to the in vivo microenvironment. J. Neurosci. 25, 11564–11576.
Pirogovsky, E., et al., 2007. Impairments in source memory for olfactory and visual stimuli in preclinical and clinical stages of Huntington's disease. J. Clin. Exp. Neuropsychol. 29, 395–404.
Pouladi, M.A., et al., 2009. Prevention of depressive behaviour in the YAC128 mouse model of Huntington disease by mutation at residue 586 of huntingtin. Brain 132, 919–932.
Rajkowska, G., et al., 1998. Neuronal and glial somal size in the prefrontal cortex: a postmortem morphometric study of schizophrenia and Huntington disease. Arch. Gen. Psychiatry 55, 215–224.
Reddy, P.H., et al., 1998. Behavioural abnormalities and selective neuronal loss in HD transgenic mice expressing mutated full-length HD cDNA. Nat. Genet. 20, 198–202.
Rigamonti, D., et al., 2001. Huntingtin's neuroprotective activity occurs via inhibition of procaspase-9 processing. J. Biol. Chem. 276, 14545–14548.
Ross, C.A., et al., 2014. Determinants of functional disability in Huntington's disease: role of cognitive and motor dysfunction. Mov. Disord. 29, 1351–1358.
Sanchez, I., et al., 1999a. Caspase-8 is required for cell death induced by expanded polyglutamine repeats. Neuron 22, 623–633.
Sanchez, I., et al., 1999b. Caspase-8 is required for cell death induced by expanded polyglutamine repeats. Neuron 22, 623–633.
Sathasivam, K., et al., 2001. Centrosome disorganization in fibroblast cultures derived from R6/2 Huntington's disease (HD) transgenic mice and HD patients. Hum. Mol. Genet. 10, 2425–2435.
Servello, A., et al., 2015. Olfactory dysfunction, olfactory bulb volume and Alzheimer's Disease: is there a correlation? A pilot Study1. J. Alzheimers Dis. 48, 395–402.
Shimohata, T., et al., 2000. Interaction of expanded polyglutamine stretches with nuclear transcription factors leads to aberrant transcriptional regulation in polyglutamine diseases. Neuropathology 20, 326–333.
Simpson, J.M., et al., 2011. Altered adult hippocampal neurogenesis in the YAC128 transgenic mouse model of Huntington disease. Neurobiol. Dis. 41, 249–260.
Singer, E., et al., 2017. Reduced cell size, chromosomal aberration and altered proliferation rates are characteristics and confounding factors in the STHdh cell model of Huntington disease. Sci. Rep. 7, 16880.
Smail, S., et al., 2016. Increased olfactory bulb BDNF expression does not rescue deficits in olfactory neurogenesis in the Huntington's Disease R6/2 Mouse. Chem. Senses 41, 221–232.
Squitieri, F., et al., 2003. Homozygosity for CAG mutation in Huntington disease is associated with a more severe clinical course. Brain 126, 946–955.
Steffan, J.S., et al., 2000. The Huntington's disease protein interacts with p53 and CREB-binding protein and represses transcription. Proc. Natl. Acad. Sci. U. S. A. 97, 6763–6768.
Tabrizi, S.J., et al., 2009. Biological and clinical manifestations of Huntington's disease in the longitudinal TRACK-HD study: cross-sectional analysis of baseline data. Lancet Neurol. 8, 791–801.
ter Laak, H.J., et al., 1994. The olfactory bulb in Alzheimer disease: a morphologic study of neuron loss, tangles, and senile plaques in relation to olfaction. Alzheimer Dis. Assoc. Disord. 8, 38–48.
Thomann, P.A., et al., 2009. MRI-derived atrophy of the olfactory bulb and tract in mild cognitive impairment and Alzheimer's disease. J. Alzheimers Dis. 17, 213–221.
Toulmond, S., et al., 2004. Neuroprotective effects of M826, a reversible caspase-3 inhibitor, in the rat malonate model of Huntington's disease. Br. J. Pharmacol. 141, 689–697.
U, M., et al., 2001. Extended polyglutamine selectively interacts with caspase-8 and -10 in nuclear aggregates. Cell Death Differ. 8, 377–386.
Uribe, V., et al., 2012. Rescue from excitotoxicity and axonal degeneration accompanied by age-dependent behavioral and neuroanatomical alterations in caspase-6-deficient mice. Hum. Mol. Genet. 21, 1954–1967.
Vilchez, D., et al., 2014. The role of protein clearance mechanisms in organismal ageing and age-related diseases. Nat. Commun. 5, 5659.
Wang, J., et al., 2011. Association of olfactory bulb volume and olfactory sulcus depth with olfactory function in patients with Parkinson disease. AJNR Am. J. Neuroradiol. 32, 677–681.
Wanker, E.E., 2002. Hip1 and Hippi participate in a novel cell death-signaling pathway. Dev. Cell 2, 126–128.
Warby, S.C., et al., 2008. Activated caspase-6 and caspase-6-cleaved fragments of huntingtin specifically colocalize in the nucleus. Hum. Mol. Genet. 17, 2390–2404.
Wellington, C.L., et al., 2002a. Caspase cleavage of mutant huntingtin precedes neurodegeneration in Huntington's disease. J. Neurosci. 22, 7862–7872.
Wellington, C.L., et al., 2002b. Caspase cleavage of mutant huntingtin precedes neurodegeneration in Huntington's disease. J. Neurosci. 22, 7862–7872.
Wirths, O., 2017. Altered neurogenesis in mouse models of Alzheimer disease. Neurogenesis (Austin) 4, e1327002.
Wong, B.K., et al., 2015. Partial rescue of some features of Huntington disease in the genetic absence of caspase-6 in YAC128 mice. Neurobiol. Dis. 76, 24–36.
Yamaguchi, M., et al., 2013. Reorganization of neuronal circuits of the central olfactory system during postprandial sleep. Front. Neural Circuits. 7, 132.
Yan, X.X., et al., 2001. Expression of active caspase-3 in mitotic and postmitotic cells of the rat forebrain. J. Comp. Neurol. 433, 4–22.
Youssef, I., et al., 2008. N-truncated amyloid-beta oligomers induce learning impairment and neuronal apoptosis. Neurobiol. Aging 29, 1319–1333.
Yu-Taeger, L., et al., 2012. A novel BACHD transgenic rat exhibits characteristic neuropathological features of Huntington disease. J. Neurosci. 32, 15426–15438.
Yu-Taeger, L., et al., 2017. Dysregulation of gene expression in the striatum of BACHD rats expressing full-length mutant huntingtin and associated abnormalities on molecular and protein levels. Neuropharmacology 117, 260–272.